# Momentum spread of spontaneously decaying cold gas in thermal radiation

C. H. Raymond Ooi,* Karl-Peter Marzlin,† and Jürgen Audretsch‡
*Fachbereich Physik der Universität Konstanz, Fach M674, D-78457 Konstanz, Germany*
(Received 17 December 2001; published 26 December 2002)

We study the quantum dynamics of the center-of-mass momentum distribution for the populations of a cold gas with two-level system undergoing spontaneous decay and coupled to a Markovian thermal reservoir at arbitrary temperature. We derive the momentum-convolutionless coupled equations for momentum Fourier transform of the populations which can be easily solved numerically and analytically for a specific internal scheme and for zero-temperature cases. The time and momentum evolutions of the populations are obtained by inverse Fourier transform. The momentum spread and the center-of-mass entropy across one momentum dimension are computed and compared for different internal schemes, between zero-temperature and finite-temperature cases and between $\pi$ and $\sigma_{\pm}$ transitions. For initial subrecoil momentum width, the $\sigma_{\pm}$ transition displays a two-peak feature. Our results well describe the momentum spread dynamics of cold gas in thermal radiation at early time and complement the results based on Fokker-Planck equation.

DOI: 10.1103/PhysRevA.66.063413 PACS number(s): 42.50.Vk, 42.50.Lc

## I. INTRODUCTION

The theory of spontaneous emissions without quantization of the center-of-mass (c.m.) motion has been developed long ago [1] based on the master equation. In the last two decades, the momentum transfer between photons and a particle in a radiative processes has been practically used to manipulate the motion of particles in laser light [2]. This is the concept behind the development of laser cooling [3] and atom optics [4]. In laser cooling, spontaneous emission is the dissipative mechanism which removes the entropy from a gas. The full quantum theory of optical laser cooling of atoms has been developed by neglecting the contribution of the thermal photons from the surrounding [5]. This is justified for optical transition occurring in atoms. For radiative transition at room temperature in the infrared frequency and below, the mean thermal photon number $\bar{n}$ may be non-negligible. For optically thick media, there is an additional source of incoherent radiation with thermal nature from radiation trapping of the spontaneous emitted photons from other particles [6]. Incoherent thermal excitations would have equally important effects as free spontaneous emissions on the momentum distribution of an ensemble of gas. This is the case of a typical molecular gas, where fluorescence in the infrared and even microwave regimes are unavoidable. The typical infrared photon momentum is only about 10–50 times smaller than an optical photon momentum and the momentum spread from spontaneous decay would be significant compared to the momentum width for ultracold gas.

The momentum spread dynamics from spontaneous emissions in thermal radiation has been developed by Dalibard and Cohen-Tannoudji *et al.* in Ref. [11] in the ''hot gas'' regime where the condition $|\mathbf{P}| \gg |\hbar\mathbf{k}|$ enables perturbative expansions in orders of $\hbar\mathbf{k}$, resulting in the Fokker-Planck equation. From the perspective of the booming research in cold gases, it would be interesting to investigate the nature of the momentum spreading from spontaneous emissions of a cold gas. In this paper, we restrict our considerations to the dilute and cold gas where the momentum width of the distribution is sufficiently narrow (in the order of recoil momentum) such that $(|\mathbf{P}| \ll Mc)$. This enables us to derive accurate theoretical solutions for finite or zero thermal radiation temperature and study the c.m. momentum spreading from the spontaneous decay. The results are also valid in the regime $|\mathbf{P}| \lesssim |\hbar\mathbf{k}|$ which is complementary to the regime described by the Fokker-Planck equation .

We develop the theory starting from the master equation with quantization of the c.m. momentum and derive the generalized Bloch equations for the populations (presented in Appendix A). In Sec. II, we show that the cold gas regime enables the Bloch equations to be expressed in closed form. Convolutionless first-order coupled differential equations are obtained by Fourier transform, which are easily solved numerically for the populations in time and momentum domains for arbitrary initial distribution by numerical integration followed by inverse fast Fourier transform. Analytical solutions of the populations in the time domain and the momentum Fourier-transform domain are obtained for a specific internal scheme. We also derive the transient solutions of the momentum-summed populations for the general case. In Sec. III analytical expressions are obtained for the populations without the thermal radiation for the initial Gaussian distribution. In Sec. IV the results for pure two-level system are presented. Expressions for the steady-state momentum distributions, momentum-summed populations and internal entropy are also derived. The c.m. entropy is computed from the probability momentum distribution while the internal entropy from the momentum-summed populations (see Appendix B). The computed results are discussed in Sec. V. Finally, in Sec. VI we compare valid range of our results with that obtained from the Fokker-Planck equation for hot gas regime.

*Electronic address: ooi@spock.physik.uni-konstanz.de
†Electronic address: Peter.Marzlin@uni-konstanz.de
‡Electronic address: Juergen.Audretsch@uni-konstanz.de

 

## II. COLD GAS IN THERMAL RADIATION

The generalized Bloch equations for momentum and time-dependent populations of a single excited state and three degenerate ground states, $j$ coupled to thermal radiation with the Born-Markov, dipole and rotating wave approximations are given by

$$\frac{\partial \rho_{ee}(\mathbf{P},t)}{\partial t} = \Gamma \frac{3}{8\pi} \int d\omega \frac{\omega^3}{{\omega_o}^3} \int_0^{2\pi} d\phi \int_0^{\pi} d\theta \sum_j \sum_{q=0,\pm 1} C_{q,j}^2 N_q(\theta)\, \delta(\Delta_{\mathbf{kP}}^{+}) \left\{ -(\overline{n}(\omega)+1)\rho_{ee}(\mathbf{P},t) + \overline{n}(\omega)\rho_{jj}\left( \mathbf{P} - \hat{\kappa}\frac{\hbar\omega}{c}, t \right) \right\},$$

$$\frac{\partial \rho_{jj}(\mathbf{P},t)}{\partial t} = \Gamma \frac{3}{8\pi} \int d\omega \frac{\omega^3}{{\omega_o}^3} \int_0^{2\pi} d\phi \int_0^{\pi} d\theta \sum_{q=0,\pm 1} C_{q,j}^2 N_q(\theta)\, \delta(\Delta_{\mathbf{kP}}^{-}) \left\{ -\overline{n}(\omega)\rho_{jj}(\mathbf{P},t) + [\overline{n}(\omega)+1]\rho_{ee}\left( \mathbf{P} + \hat{\kappa}\frac{\hbar\omega}{c}, t \right) \right\}, \quad (1)$$

where $\Gamma \doteq (d_o^2 {\omega_o}^3/3\varepsilon_o \hbar \pi c^3)$, $\overline{n}(\omega) \doteq (e^{\hbar\omega/k_B T}-1)^{-1}$, $N_q(\theta) \doteq \delta_{q0}\sin^3\theta + \delta_{q\pm}(\sin\theta - \frac{1}{2}\sin^3\theta)$, $\Delta_{j\mathbf{kP}}^{\pm} \doteq \omega - \omega_{oj} - \mathbf{P}\cdot\hat{\kappa}\omega/Mc \pm \hbar\omega^2/2Mc^2$, and $\hat{\kappa} \doteq (\sin\theta\cos\phi, \sin\theta\sin\phi, \cos\theta)$. The detailed derivation of Eqs. (1) starting from the master equation is presented in Appendix A. The right-hand side of Eqs. (1) are convoluted in the frequency and angular variables in a complicated manner due to the angular dependence in the $\delta$ function and cannot be expressed exactly in a closed form.

We consider a distribution of cold gas ($|\mathbf{P}| \ll Mc$) where the maximum Doppler frequency, $|P_{\max}\omega/Mc|$ is negligible. For the typical transition frequency at optical frequency and below, $\omega_o \lesssim 10^{16}\ \mathrm{s}^{-1}$ and particle mass of $M \gtrsim 10$ a.m.u., the corresponding recoil frequency $\omega_r \sim \hbar\omega_o^2/2Mc^2 \lesssim 10^{-10}\omega_o$ is negligibly small compared to the transition frequency $\omega_o$. Therefore, the contributions of the Doppler frequency and recoil frequency in $\delta(\omega - \omega_o - \omega_{\mathbf{P}} \pm \omega_r)$ can be disregarded and Eqs. (1) is reduced to a simpler form

$$\frac{\partial \rho_{ee}(\mathbf{P},t)}{\partial t} = -\Gamma(\overline{n}+1)\rho_{ee}(\mathbf{P},t) + \Gamma\overline{n}\sum_{q=0,\pm} \alpha_q \tilde{\rho}_{qq}(\mathbf{P},t),$$

$$\frac{\partial \rho_{qq}(\mathbf{P},t)}{\partial t} = \Gamma(\overline{n}+1)\alpha_q \tilde{\rho}_{ee}^{q}(\mathbf{P},t) - \Gamma\overline{n}\alpha_q \rho_{qq}(\mathbf{P},t), \quad (2)$$

with the definitions

$$\tilde{\rho}_{qq}(\mathbf{P},t) \doteq \frac{3}{8\pi}\int_0^{2\pi} d\phi \int_0^{\pi} d\theta N_q(\theta)\rho_{qq}(\mathbf{P} - \hat{\kappa}\hbar k_o, t),$$

$$\tilde{\rho}_{ee}^{q}(\mathbf{P},t) \doteq \frac{3}{8\pi}\int_0^{2\pi} d\phi \int_0^{\pi} d\theta N_q(\theta)\rho_{ee}(\mathbf{P} + \hat{\kappa}\hbar k_o, t), \quad (3)$$

where $\alpha_q \doteq \Sigma_j C_{q,j}^2 \delta_{M_j, M_e+q}$ is the transition coefficient, with normalization $\Sigma_q \alpha_q = 1$ and $k_o \doteq \omega_o/c$. We have used $\int_0^{2\pi} d\phi \int_0^{\pi} d\theta N_q(\theta) = (8\pi/3)$ and the one-to-one correspondence between the state index $j$ and the transition index $q$ from $M_j = M_e + q$. The convolution integrals $\tilde{\rho}_{gg}(\mathbf{P},t)$ and $\tilde{\rho}_{ee}(\mathbf{P},t)$ contain the contributions of all momentum families within $\hbar k_o$ radius from $\mathbf{P}$ as the result of momentum recoils in all directions from incoherent photon absorptions and emissions, respectively.

Now, we can perform the Fourier transform on Eqs. (2) defined by $\Pi_{ee(qq)}(\mathbf{Q},t) \doteq F\{\rho_{ee(qq)}(\mathbf{P},t)\} = \int_{-\infty}^{\infty} \rho_{ee(qq)}(\mathbf{P},t) e^{-i\mathbf{P}\cdot Q} d^3P$ and obtain a closed set of coupled linear equations

$$\frac{\partial \Pi_{ee}(\mathbf{Q},t)}{\partial t} = -\Gamma(\overline{n}+1)\Pi_{ee}(\mathbf{Q},t) + \Gamma\overline{n}\sum_q \alpha_q f_q(-\mathbf{Q})\Pi_{qq}(\mathbf{Q},t),$$

$$\frac{\partial \Pi_{qq}(\mathbf{Q},t)}{\partial t} = \Gamma(\overline{n}+1)\alpha_q f_q(\mathbf{Q})\Pi_{ee}(\mathbf{Q},t) - \alpha_q \Gamma\overline{n}\Pi_{qq}(\mathbf{Q},t), \quad (4)$$

where $f(\pm\mathbf{Q}) \doteq 3/8\pi \int_0^{2\pi} d\phi \int_0^{\pi} d\theta N_q(\theta) e^{\pm i\mathbf{Q}\cdot\hbar\mathbf{k}_o}$.

Next, we evaluate the function $f_q(\pm\mathbf{Q})$. By using $Q_x\cos\phi + Q_y\sin\phi \equiv A\cos(\phi - \alpha)$ with $A\cos\alpha = Q_x$, $A\sin\alpha = Q_y$, $A = \sqrt{Q_x^2 + Q_y^2}$ and $\int_0^{2\pi} e^{\pm iB\cos(\phi-\alpha)} d\phi = 2\pi J_0(B)$ with $B = A\hbar k_o \sin\theta$, we can rewrite

$$f_q(\pm\mathbf{Q}) \doteq \frac{3}{8\pi}\int_0^{\pi} d\theta N_q(\theta) \times 2\pi J_0(\sqrt{Q_x^2+Q_y^2}\hbar k_o \sin\theta) e^{\pm iQ_z\hbar k_o \cos\theta}. \quad (5)$$

By replacing $S \doteq \hbar k_o \cos\theta$, Eq. (5) becomes

$$f_q(\mathbf{Q}) \doteq \int_{-\hbar k_o}^{\hbar k_o} N_q'(S) \times J_0\left[ \sqrt{Q_x^2+Q_y^2}\hbar k_o \sqrt{1 - \left(\frac{S}{\hbar k_o}\right)^2} \right] e^{iQ_z S} dS, \quad (6)$$

where $f(-\mathbf{Q}) = f(\mathbf{Q})$ is an even function since $J_0$ and $N_q'(S) \doteq (3/4\hbar k_o)[1 - (S/\hbar k_o)^2]\delta_{q0} + (3/8\hbar k_o)[1 + (S/\hbar k_o)^2]\delta_{q\pm}$ are even functions of $S$.

Equations (4) describe the time evolution of the Fourier transform of the populations for ultracold gas exposed to thermal radiation and can be solved for $\Pi_{ee(qq)}(\mathbf{Q},t)$ numerically and then numerically perform an inverse Fourier transform to obtain $\rho_{ee(qq)}(\mathbf{P},t)$. We can also proceed with the

Laplace transform of Eqs. (4) using $\Pi_{ee(qq)}(\mathbf{Q},s) \doteq L\{\Pi_{ee(qq)}(\mathbf{Q},t)\} = \int_0^\infty \Pi_{ee(qq)}(\mathbf{Q},t)e^{-st}dt$ and solve for $\Pi_{ee(qq)}(\mathbf{Q},s)$ analytically. However, in general case where all the coefficients are different $\alpha_- \neq \alpha_0 \neq \alpha_+$, the inverse Laplace transform of $\Pi_{ee(qq)}(\mathbf{Q},s)$ to $\Pi_{ee(qq)}(\mathbf{Q},t)$ are algebraically too cumbersome. This is so even for the case of 'symmetric' transition coefficients $\alpha_- = \alpha_+$, and $2\alpha_\pm + \alpha_0 = 1$, which applies when $M_e = 0$.

### A. Analytical solutions with same transition coefficients

For the case where the excited state is $|J_e = 0, M_e = 0\rangle$ and the ground states are $|J_q = 1, M_q = 0, \pm 1\rangle$ all the transition coefficients are the same, $\alpha_q = \alpha = \frac{1}{3}$. This applies to most atoms, and to the spinless molecules in ground electronic state $^1\Sigma_0$. Thus, Eqs. (4) yield analytical solutions

$$\Pi_{ee}(\mathbf{Q},t) = \Pi_{ee}(\mathbf{Q},0)e^{-\gamma t}\left(\cosh zt - \frac{y}{z}\sinh zt\right) + \sum_q f_q(\mathbf{Q})\Pi_{qq}(\mathbf{Q},0)\frac{\alpha\Gamma\bar{n}}{z}e^{-\gamma t}\sinh zt,$$

$$\Pi_{kk}(\mathbf{Q},t) = \Pi_{ee}(\mathbf{Q},0)\frac{\alpha\Gamma(\bar{n}+1)f_k(\mathbf{Q})}{z}e^{-\gamma t}\sinh zt + \Pi_{kk}(\mathbf{Q},0)e^{-\alpha\Gamma\bar{n}t} + \frac{f_k(\mathbf{Q})}{2f_\pm^2(\mathbf{Q}) + f_0^2(\mathbf{Q})}\left\{\sum_q f_q(\mathbf{Q})\Pi_{qq}(\mathbf{Q},0)\right\} \times \left\{e^{-\gamma t}\left(\frac{y}{z}\sinh zt + \cosh zt\right) - e^{-\alpha\Gamma\bar{n}t}\right\}, \quad (7)$$

where $\gamma \doteq \frac{1}{2}\Gamma(\bar{n}(\alpha+1)+1)$, $z(\mathbf{Q})^2 \doteq \Gamma^2\alpha^2\bar{n}(\bar{n}+1)\{2f_\pm^2(\mathbf{Q}) + f_0^2(\mathbf{Q})\} + y^2$, and $y \doteq \frac{1}{2}\Gamma((1-\alpha)\bar{n}+1)$.

Three-dimensional populations distributions in momentum space can be obtained by numerically inverse Fourier transforming Eqs. (4). However, it is not possible to display a $3d$ plot of the momentum distribution in three dimensional momentum space. The physics of the decay dynamics can be seen more clearly from a specific direction in momentum space.

### B. One-dimensional momentum dependence

We shall investigate the momentum spread along the $z$ direction, which is defined as the quantization axis. We compare the cases for $\pi$ transition ($\Delta M = 0$) and for $\sigma\pm$ transition ($\Delta M = \pm 1$). The $z$-momentum dependent populations $\pi_{ee}(P_z,t), \pi_{qq}(P_z,t)$ are obtained by tracing out the $x$ and $y$ momentum components [5] using

$$\pi_{aa}(P_z,t) = \int_{-\infty}^{\infty} dP_x \int_{-\infty}^{\infty} dP_y \rho_{aa}(P_x,P_y,P_z,t) = \frac{1}{2\pi}\int_{-\infty}^{\infty} \Pi_{aa}(0,0,Q_z,t)e^{iP_zQ_z}dQ_z,$$

$$\tilde{\pi}_{aa}(P_z,t) = \frac{1}{2\pi}\int_{-\infty}^{\infty} f(\pm Q_z)\Pi_{aa}(0,0,Q_z,t)e^{iP_zQ_z}dQ_z. \quad (8)$$

This is equivalent to setting $Q_x = Q_y = 0$ in Eqs. (5) and (6), which give

$$f_q(Q) \doteq \frac{3}{4}\int_0^\pi N_q(\theta)e^{iQ\hbar k_o\cos\theta}d\theta = \int_{-\hbar k_o}^{\hbar k_o} N_q'(S)e^{iSQ}dS,$$

$$f_\pm(Q) \doteq \frac{3}{2}\frac{\sin y}{y} - \frac{1}{2}f_0(y),$$

$$f_0(Q) \doteq 3\left(\frac{\sin y}{y^3} - \frac{\cos y}{y^2}\right) = j_0(y) + j_2(y) = \sqrt{\frac{\pi}{2y}}\{J_{1/2}(y) + J_{5/2}(y)\}, \quad (9)$$

where $y \doteq Q\hbar k_o$ and the subscript $z$ has been dropped.

From the definitions in Eqs. (8), we obtain the coupled equations,

$$\frac{d}{dt}\pi_{ee}(P,t) = -\Gamma(\bar{n}+1)\pi_{ee}(P,t) + \Gamma\bar{n}\sum_q \alpha_q\tilde{\pi}_{qq}(P,t),$$

$$\frac{d}{dt}\pi_{qq}(P,t) = \alpha_q\Gamma(\bar{n}+1)\tilde{\pi}_{ee}^q(P,t) - \alpha_q\Gamma\bar{n}\pi_{qq}(P,t), \quad (10)$$

where $\tilde{\pi}_{ee}^q(P,t) \doteq \int_{-\hbar k_o}^{\hbar k_o} N_q(S)\pi_{ee}(P+S,t)dS$ and $\tilde{\pi}_{qq}(P,t) \doteq \int_{-\hbar k_o}^{\hbar k_o} N_q(S)\pi_{qq}(P-S,t)dS$. For the case $\alpha_q = \alpha = \frac{1}{3}$, solutions of Eqs. (10) are obtained by inverse Fourier transforming the Eqs. (7) upon setting $\mathbf{Q} \to Q_z$. When $\bar{n} = 0$, Eqs. (10) reduce to that of Ref. [5].

### C. Analytical solutions of momentum-summed populations

The *external(momentum)-summed* populations are defined as $\pi_{aa}(t) \doteq \int_{-\infty}^{\infty}\pi_{aa}(\mathbf{P},t)d^3P = \Pi_{aa}(\mathbf{Q=0},t)$. It follows that $f_q(\mathbf{0}) = \int_{-\hbar k_o}^{\hbar k_o} N_q(S)dS = 1$. For the case of $M_e = 0$, we have the symmetric case where $\alpha_\pm = \alpha$, and $\alpha_0 = 1 - 2\alpha_\pm$. We can solve Eqs. (10) analytically for the time evolution of the populations,

$$\pi_{ee}(t)=\pi_{ee}(0)\left(e^{-\gamma t}\cosh zt-\Gamma\frac{(\alpha\bar{n}+1)}{2z}e^{-\gamma t}\sinh zt\right)+\{\alpha\pi_{--}(0)+\alpha\pi_{++}(0)+(1-2\alpha)\pi_{00}(0)\}\frac{\Gamma\bar{n}}{z}e^{-\gamma t}\sinh zt+\Gamma^2\bar{n}^2\alpha\times(1-2\alpha)F(0,t),$$

$$\pi_{--}(t)=\pi_{ee}(0)\frac{\Gamma(\bar{n}+1)\alpha}{z}e^{-\gamma t}\sinh zt+\pi_{--}(0)e^{-\alpha\Gamma\bar{n}t}+\Gamma^2\bar{n}(\bar{n}+1)\alpha(1-2\alpha)F(0,t)+\{\pi_{++}(0)+\pi_{--}(0)\}\alpha(3\alpha-1)\Gamma^2\bar{n}(\bar{n}+1)F(\alpha\Gamma\bar{n},t),$$

$$\pi_{00}(t)=\pi_{ee}(0)\frac{\Gamma(\bar{n}+1)(1-2\alpha)}{z}e^{-\gamma t}\sinh zt+\pi_{00}(0)\times\left(e^{-\gamma t}\cosh zt+\frac{1}{2}\Gamma\frac{(1+3\alpha\bar{n})}{z}e^{-\gamma t}\sinh zt\right)+\frac{\bar{n}+1}{4\bar{n}+3}\left\{1-e^{-\gamma t}\left(\cosh zt+\frac{\gamma}{z}\sinh zt\right)\right\},$$

$$\pi_{++}(t)=\pi_{ee}(0)\frac{\Gamma(\bar{n}+1)\alpha}{z}e^{-\gamma t}\sinh zt+\pi_{++}(0)e^{-\alpha\Gamma\bar{n}t}+\Gamma^2\bar{n}(\bar{n}+1)\alpha(1-2\alpha)F(0,t)+\{\pi_{++}(0)+\pi_{--}(0)\}\alpha(3\alpha-1)\Gamma^2\bar{n}(\bar{n}+1)F(\alpha\Gamma\bar{n},t),\tag{11}$$

where $F(A,t)\doteq 1/[z^2-(\gamma-A)^2]\{e^{-\gamma t}[(\gamma-A)/z)\sinh zt+\cosh zt]-e^{-At}\}$, $F(0,t)\doteq[1/(z^2-\gamma^2)]\{e^{-\gamma t}[(\gamma/z)\sinh zt+\cosh zt]-1\}$, $\gamma\doteq\frac{1}{2}\Gamma[\bar{n}(2-\alpha_{\pm})+1]$, and $z^2\doteq[\alpha_{\pm}\bar{n}(-5\bar{n}-\frac{7}{2}+\frac{33}{4}\alpha_{\pm}\bar{n}+6\alpha_{\pm})+\bar{n}(\bar{n}+1)+\frac{1}{4}]\Gamma^2$.

When all coefficients are the same $\alpha_{\pm}=\alpha=\alpha_0=\frac{1}{3}$, Eqs. (11) reduce to

$$\pi_{ee}(t)=e^{-(4/3\bar{n}+1)\Gamma t}\pi_{ee}(0)+\frac{\bar{n}}{4\bar{n}+3}(1-e^{-(4/3\bar{n}+1)\Gamma t}),$$

$$\pi_{qq}(t)=\frac{(\bar{n}+1)}{(4\bar{n}+3)}+\frac{\bar{n}}{3(4\bar{n}+3)}e^{-(4/3\bar{n}+1)\Gamma t}-\frac{1}{3}\pi_{ee}(0)e^{-(4/3\bar{n}+1)\Gamma t},\tag{12}$$

where $\pi_{qq}(t)=\pi_{--}(t)=\pi_{00}(t)=\pi_{++}(t)$ and $\pi_{ee}(t)+3\pi_{qq}(t)=1$. We obtain the same results from Eqs. (7) by setting $f_k(\mathbf{Q})\to 1$.

The steady-state solutions for "identical" ground states are obtained from Eqs. (12) as $\pi_{ee,st}=(\bar{n}/4\bar{n}+3)=1/(1+3e^{x})$ and $\pi_{qq,st}=(\bar{n}+1)/(4\bar{n}+3)=e^{x}/(1+3e^{x})$. The ratio of the excited-state population to the each ground state has the Maxwell-Boltzmann distribution. The equilibrium entropy is

$$S_{i,st}=k_B\ln(1+3e^{\hbar\omega_o/k_BT})-\left(\frac{\hbar\omega_o}{T}\right)(\tfrac{1}{3}e^{-\hbar\omega_o/k_BT}+1)^{-1}.\tag{13}$$

## III. ZERO TEMPERATURE CASE

For $\bar{n}=0$ with general transition coefficients $\alpha_q$, Eqs. (2) lead to the decoupled exact solutions for the populations

$$\pi_{ee}(\mathbf{P},t)=\pi_{ee}(\mathbf{P},0)e^{-\Gamma t},$$
$$\pi_{qq}(\mathbf{P},t)=\pi_{qq}(\mathbf{P},0)+D_q(\mathbf{P})(1-e^{-\Gamma t}),\tag{14}$$

where $D_q(\mathbf{P})\doteq\alpha_q\frac{1}{(2\pi)^{3/2}}\int_{-\infty}^{\infty}e^{i\mathbf{P}\cdot Q}\Pi_{ee}(\mathbf{Q},0)f_q(\mathbf{Q})d^3Q$.

For one-dimensional momentum dependence, we have

$$D_q(P)=\alpha_q\frac{1}{\sqrt{2\pi}}\int_{-\infty}^{\infty}e^{iPQ}\Pi_{ee}(Q,0)f_q(Q)dQ,$$
$$=\alpha_q\frac{1}{\sqrt{2\pi}}\int_{-\infty}^{\infty}e^{iPQ}\Pi_{ee}(Q,0)dQ\int_{-\hbar k_o}^{\hbar k_o}e^{iSQ}N_q'(S)dS,$$
$$=\alpha_q\int_{-\hbar k_o}^{\hbar k_o}N_q'(S)\pi_{ee}(P+S,0)dS,\tag{15}$$

with the notations defined in Eqs. (9).

By assuming the initial population distribution to be Gaussian, $\pi_{ee}(P,0)=(1/\sqrt{\pi}\sigma)e^{-P^2/\sigma^2}$, we obtain the analytical expressions for $D_q(P)$,

$$D_0(P)\doteq\frac{3\bar{\sigma}}{8\sqrt{\pi}(\hbar k_o)}[e^{[-(-1+p)^2/\bar{\sigma}^2]}(1+p)+e^{-[(1+p)^2/\bar{\sigma}^2]}(1-p)],$$
$$+\frac{3}{16(\hbar k_o)}(2p^2-2+\bar{\sigma}^2)\times\left[\mathrm{erf}\left(\frac{-1+p}{\bar{\sigma}}\right)-\mathrm{erf}\left(\frac{1+p}{\bar{\sigma}}\right)\right],\tag{16}$$

$$D_{\pm}(P)\doteq-\frac{3\bar{\sigma}}{16\sqrt{\pi}(\hbar k_o)}[e^{-[(-1+p)^2/\bar{\sigma}^2]}(1+p)+e^{-[(1+p)^2/\bar{\sigma}^2]}(1-p)]$$
$$-\frac{3}{16(\hbar k_o)}(p^2+1+\bar{\sigma}^2/2)\times\left[\mathrm{erf}\left(\frac{-1+p}{\bar{\sigma}}\right)-\mathrm{erf}\left(\frac{1+p}{\bar{\sigma}}\right)\right],\tag{17}$$

where $\bar{\sigma}\doteq\sigma/\hbar k_o$, $p\doteq P/\hbar k_o$.

The steady-state momentum distribution is $f(\mathbf{P})_{st}=\Sigma_q\{\pi_{qq}(\mathbf{P},0)+D_q(\mathbf{P})\}$ while the corresponding momentum-summed populations are $\pi_{ee,st}\rightarrow 0, \pi_{qq,st}\rightarrow \pi_{qq}(0)+\alpha_q\pi_{ee}(0)$.

## IV. PURE TWO-LEVEL SYSTEM

For the pure two-level system, the momentum spread is due to either $\pi$ or $\sigma$ transition and not both. This enables us to distinguish the nature of momentum spread between the two types of transitions. The results for pure two-state system in thermal radiation are easily obtained from Eqs. (4) by setting $\alpha_q\rightarrow 1$ and $q\rightarrow g$ as

$$\Pi_{ee}(\mathbf{Q},t)=e^{-\gamma_2 t}\left\{\Pi_{ee}(\mathbf{Q},0)\left(\cosh z_2 t-\frac{\Gamma}{2z_2}\sinh z_2 t\right)+\Pi_{gg}(\mathbf{Q},0)\frac{\Gamma}{z_2}\bar{n}f_g(\mathbf{Q})\sinh z_2 t\right\},$$

$$\Pi_{gg}(\mathbf{Q},t)=e^{-\gamma_2 t}\left\{\Pi_{ee}(\mathbf{Q},0)\frac{\Gamma}{z_2}(\bar{n}+1)f_g(\mathbf{Q})\sinh z_2 t+\Pi_{gg}(\mathbf{Q},0)\left(\cosh z_2 t+\frac{\Gamma}{2z_2}\sinh z_2 t\right)\right\}, \quad (18)$$

where $f_g(\mathbf{Q})$ is defined in Eq. (6), $z_2(\mathbf{Q})\doteq\Gamma\sqrt{\bar{n}(\bar{n}+1)f_g^2(\mathbf{Q})+\frac{1}{4}}$ and $\gamma_2\doteq\frac{1}{2}\Gamma(2\bar{n}+1)$. For $\bar{n}=0$, Eqs. (18) are equivalent to Eqs. (14), except with the replacement $\alpha_q\rightarrow 1$ and $q\rightarrow g$.

The momentum-summed solutions follow from Eqs. (18):

$$\pi_{ee}(t)=\frac{1}{2}\left[1+e^{-\gamma_2 t}-\frac{(1-e^{-\gamma_2 t})}{2\bar{n}+1}\right]\pi_{ee}(0)+\frac{\bar{n}(1-e^{-\gamma_2 t})}{(2\bar{n}+1)}\pi_{gg}(0),$$

$$\pi_{gg}(t)=\frac{(\bar{n}+1)(1-e^{-\gamma_2 t})}{(2\bar{n}+1)}\pi_{ee}(0)+\frac{1}{2}\left(1+e^{-\gamma_2 t}+\frac{(1-e^{-\gamma_2 t})}{(2\bar{n}+1)}\right)\pi_{gg}(0), \quad (19)$$

where $\gamma_2\doteq\frac{1}{2}\Gamma(2\bar{n}+1)$.

At steady state, Eqs. (19) reduce to the Maxwell-Boltzmann thermal distribution for internal states [13] $\pi_{ee,st}=\bar{n}/(2\bar{n}+1)=1/(e^x+1)$ and $\pi_{gg,st}=(\bar{n}+1)/(2\bar{n}+1)=e^x/(e^x+1)$ where $x=\hbar\omega_o/k_BT$ with the corresponding internal entropy

$$S_{i,st}=k_B\ln(e^{\hbar\omega_o/k_BT}+1)-\frac{\hbar\omega_o/T}{e^{-\hbar\omega_o/k_BT}+1}, \quad (20)$$

which is of course smaller than the degenerate ground-states case, Eq. (20).

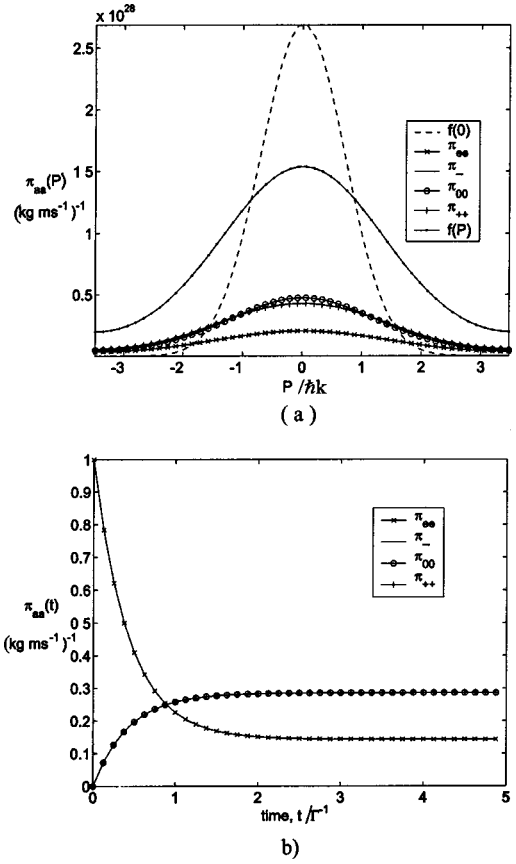


FIG. 1. Case of the same transition coefficients, $\alpha_\pm=\alpha_0=\frac{1}{3}$ (for the excited state $|J_e=0,M_e=0\rangle$ and the ground states $|J_g=1,M_q=0,\pm 1\rangle$) in thermal radiation, $\bar{n}=1$, with an initial Gaussian momentum width of $\sigma=1\hbar k\sim 2\times 10^{-29}$ kgm s$^{-1}$: (a) momentum distributions for the excited state $\pi_{ee}(P)$, ground states $\pi_{--}(P), \pi_{00}(P)$ and $\pi_{++}(P)$, and total $f(P)$ populations versus normalized momentum $P/\hbar k$ at time $t=5/\Gamma$. The figure is computed from analytical results, Eqs. (7). (b) Time evolutions of the populations (momentum summed) are computed from analytical results, Eqs. (12). [Note: The $x$ axis is in units of $\Gamma^{-1}$. The scale of $10^{28}$ on the $y$ axis is due to the normalization $\int f(P)dP=1$.]

## V. DISCUSSIONS OF COMPUTED RESULTS

We have computed the distributions along $z$-momentum component and temporal evolutions of the populations for three schemes of the two-level system with three degenerate ground states in thermal radiation, $\bar{n}=1$. The simplest one is the identical scheme (shown in Figs. 1) for excited state $|J_e=0,M_e=0\rangle$ and the ground states $|J_q=1,M_q=0,\pm 1\rangle$ with all the transition coefficients $\alpha_q=\alpha=\frac{1}{3}$. The "symmetric" scheme with $\alpha_\pm=\frac{3}{10},\alpha_0=\frac{2}{5}$ for states $|J_e=1,M_e=0\rangle$ and $|J_g=2,M_q=\pm 2,\pm 1,0\rangle$ are shown in Figs. 2. The results for the scheme with different coefficients $\alpha_-=\frac{1}{2},\alpha_0=\frac{1}{3},\alpha_+=\frac{1}{6}$ with $|J_e=\frac{1}{2},M_e=-\frac{1}{2}\rangle$ and $|J_g=\frac{3}{2},M_q=-\frac{3}{2},-\frac{1}{2},\frac{1}{2}\rangle$ are shown in Figs. 3. In computing Figs. 1(a), we have used analytical solutions of Eqs. (7), which agree very well with the results from the numerical integration of Eqs. (4). We have also verified the validity of Eqs. (12) and (11) used for computing Figs. 1(b) and 2(b), respectively.

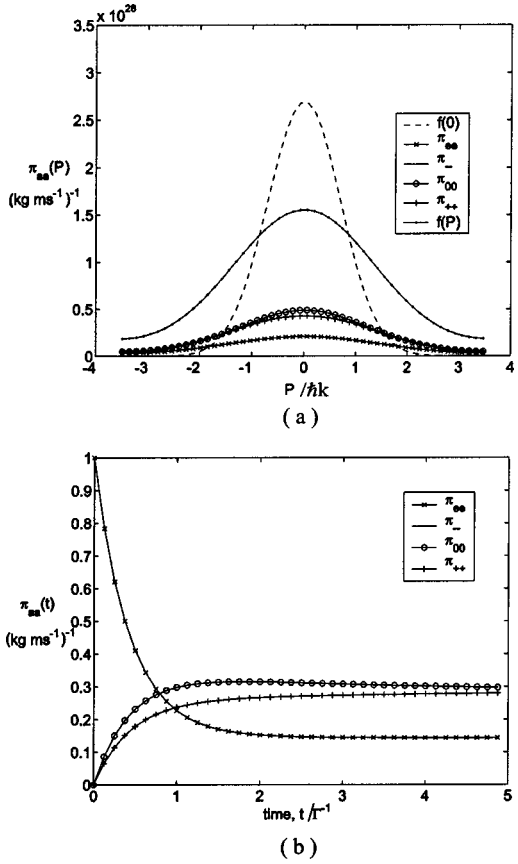


FIG. 2. Case of symmetric transition coefficients, $\alpha_{\pm}=\frac{3}{10}$, $\alpha_0=\frac{2}{5}$ in thermal radiation, $\bar{n}=1$ with initial momentum width $1\hbar k$. (a) Momentum distributions of the populations at time $t=5/\Gamma$. (b) Time evolutions of the populations (momentum summed) computed from analytical results, Eqs. (11).

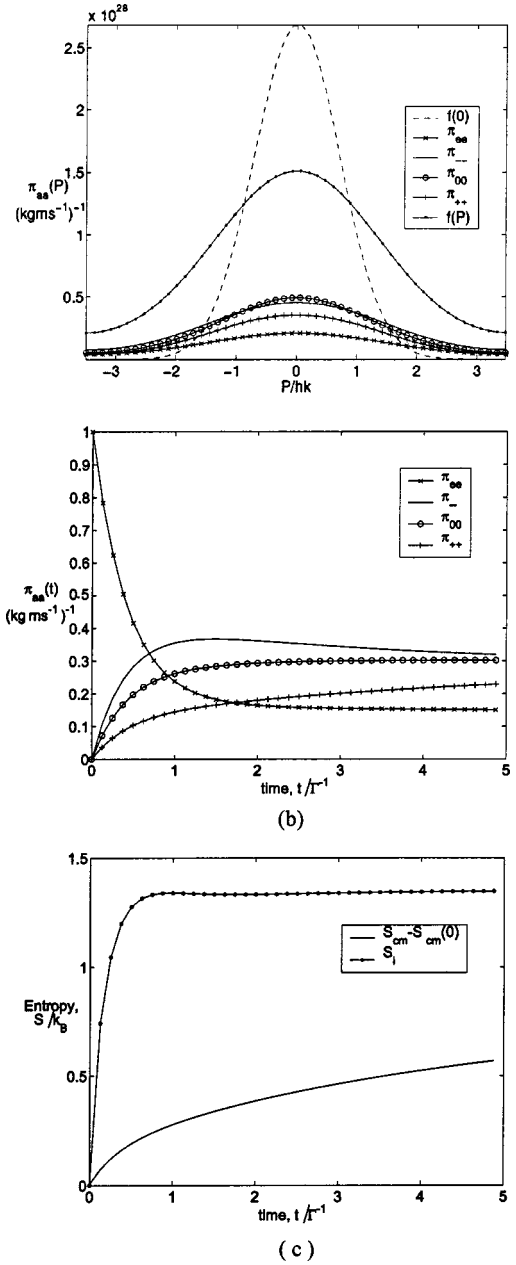


FIG. 3. Case of different transition coefficients, $\alpha_-=\frac{1}{2}$, $\alpha_0=\frac{1}{3}$, $\alpha_+=\frac{1}{6}$ for the excited state $|J_e=\frac{1}{2},M_e=-\frac{1}{2}\rangle$ and the ground states $|J_g=\frac{3}{2},M_q=-\frac{3}{2},-\frac{1}{2},\frac{1}{2}\rangle$ in thermal radiation, $\bar{n}=1$, with initial momentum width $1\hbar k$. (a) Momentum distributions of the populations at time $t=5/\Gamma$. (b) Time evolutions of the populations (momentum summed). (c) Time evolutions of the c.m. entropy difference, $S_{cm}-S_{cm}(0)$ and the internal entropy $S_i$. All results in (a), (b), and (c) are computed numerically.

As expected, the populations in all states have a momentum spread [Figs. 1(a), 2(a), 3(a)] compared to the initial total distribution $f(P,0)$ due to incoherent interaction with the thermal radiation. From Fig. 1(a), even if the transition coefficients $\alpha_q$ are the same, we see that the spreading for $\sigma$ transitions are slightly larger. This is due to the different angular dependence $N_q(\theta)$ between the $\sigma$ and $\pi$ transitions. This difference can be seen more clearly in Fig. 2(a) where $\alpha_q$ are different for the $\sigma$ and $\pi$ transitions. From Fig. 3(a), where the coefficients are different, the momentum spreads are different for different transitions.

The time evolution of the populations can be analyzed from Figs. 1(b), 2(b), and 3(b). The excited population decays exponentially, essentially unaffected by the transition coefficients of the ground states. For the same $\alpha_q$ case, the ground-state populations increases exponentially [Fig. 1(b)]. However, when $\alpha_q$ are different, the time evolution would be different and can be *nonexponential*, although the populations seem to evolve to a common equilibrium value. This is clearly seen in Fig. 3(b), where the population $\pi_{--}$ with largest coefficient $\alpha_-=\frac{1}{2}$ rises above the equilibrium value at around $t\sim 1/\Gamma$ before falling towards a converging value. This is compared to the case without thermal photons [Fig. 5(b)], where the steady-state populations are dependent on the transition coefficients $\alpha_q$ instead of the temperature.

It would be interesting to compare the momentum spreads between the $\sigma$ transition and the $\pi$ transition for the pure two-level system. The polarization of the emitted photons also affect the momentum spread. Figures 6(a) and 6(b) show that the spread is slightly larger for the $\sigma$ transition than the

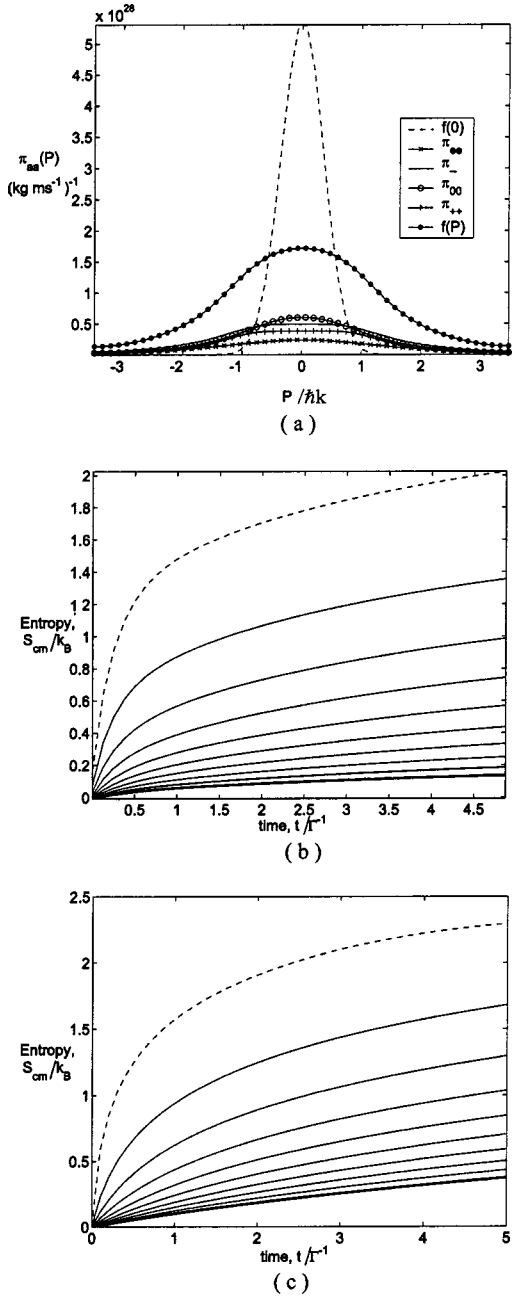


FIG. 4. Same as the case in Fig. 3 (different transition coefficients, $\alpha_-=\frac{1}{2}$, $\alpha_0=\frac{1}{3}$, $\alpha_+=\frac{1}{6}$ with thermal radiation, $\overline{n}=1$). (a) Momentum distributions of the populations at time $t=5/\Gamma$ with an initial subrecoil momentum width of $0.5\hbar k$ and time evolutions of the c.m. entropy difference $S_{cm}-S_{cm}(0)$ from (b) this paper and (c) the Fokker-Planck equation [Eq. (21)] for initial Gaussian distribution.

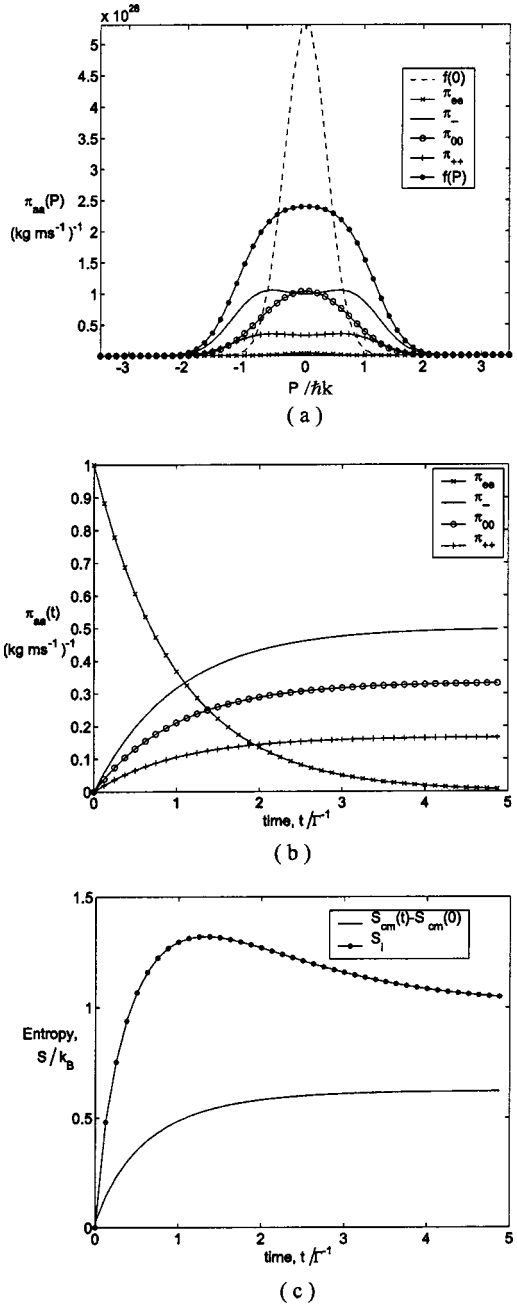


FIG. 5. Same as Fig. 4 except without thermal radiation, $\overline{n}=0$. (Initial subrecoil momentum width of $0.5\hbar k$. Different transition coefficients, $\alpha_-=\frac{1}{2}$, $\alpha_0=\frac{1}{3}$, $\alpha_+=\frac{1}{6}$.) (a) Momentum distributions of the populations at time $t=5/\Gamma$, (b) time evolutions of the populations, and (c) time evolutions of the c.m. entropy difference $S_{cm}-S_{cm}(0)$ and the internal entropy $S_i$.

$\pi$ transition. This is due to the different angular dependence of the spontaneously emitted photons ($\sin^2\theta$ for $\pi$ transition and $1-\frac{1}{2}\sin^2\theta$ for $\sigma\pm$ transitions). For $\pi$ transition, a photon tends to be emitted at right angle to the dipole (which coincides with the quantization axis) while for $\sigma$ transition, a photon tends to be emitted parallel to the dipole.

For subrecoil initial momentum width, the ground populations display a soft double-peak feature [Fig. 5(a)] and can be seen clearer in the pure two-level case [Fig. 7(a)]. This feature exists only for the $\sigma$ transition (and not in $\pi$ transition) in the absence of thermal radiation $\overline{n}=0$. It is due to the angular anisotropy of the photon emissions in the $\sigma$ transition, with higher transition probability along the $z$ axis (which coincides with quantization axis) The population around zero momentum (peak) undergoes recoil around towards $\pm\hbar k$ during spontaneous emission. The double peak feature does not show up in the presence of thermal radiation

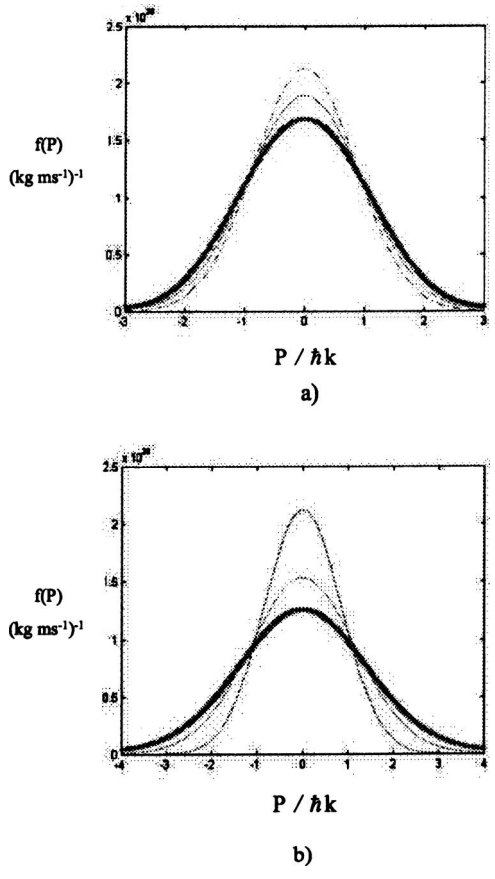


FIG. 6. Pure two-level system. Probability distribution $f(\mathbf{P})$ at $t=5/\Gamma$ for (a) case of $\bar{n}=0$ and (b) case of $\bar{n}=1$, with initial distribution (dashed line), $\pi$ transition ($q=0$, thin line), and $\sigma\pm$ transitions ($q=\pm 1$, thick line).

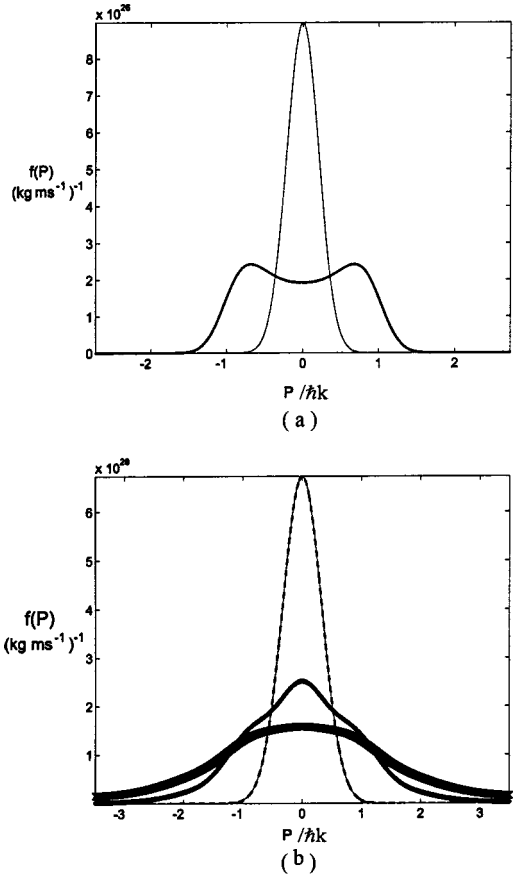


FIG. 7. Pure two-level system. Probability distribution $f(\mathbf{P})$ for $\sigma$ transitions ($q=\pm 1$) with subrecoil initial width $\sigma=0.4\hbar k_o$: (a) case $\bar{n}=0$ at $t=5/\Gamma$ for $\sigma=0.4\hbar k_o$ and (c) case $\bar{n}=1$, $\sigma=0.4\hbar k_o$ for distributions at initial (thin line), $2/\Gamma$ (line), and $5/\Gamma$ (thick line).

[Figs. 4(a) and 7(b)], since photon reabsorption repopulates the population around zero momentum and smooths out the distribution.

The time evolution of the c.m. entropy and the internal entropy are also analyzed. In thermal radiation, the internal entropy rises very fast to a maximum after about $1/\Gamma$ while the c.m. entropy increases almost logarithmically [Figs. 3(c), 4(b), 5(c)]. It is interesting to find from Fig. 4(b) that the c.m. entropy increases faster and to a larger value if the initial momentum width is smaller. The rate of entropy reduces with time. Comparison of Fig. 7(b) and Fig. 7(c) also shows qualitative correspondence between our results and that from Ref. [11]. For zero temperature, the internal entropy approaches zero [Fig. 5(c)] since all the populations decay to one internal state while the c.m. entropy begins to saturate after about two decay lifetime. Equations (14) show that the spontaneous decay does not lead to momentum spread in the excited-state population since there is no excitation from the ground state.

When thermal photons are present, the decay process is no longer purely characterized by free decay from spontaneous emission. The thermal photons induce incoherent excitations (absorption) which occur concurrently with the spontaneous emissions. Both processes contribute to give the overall momentum spread. The thermal photons act as the noise which gives the heating effect or momentum diffusion through the fluctuation-dissipation mechanism in a decay process. The excited population shrinks with a slight momentum spread while the ground population increases with greater momentum spread than in the case of $\bar{n}=0$. On overall, the momentum spread in the probability distribution is larger for $\bar{n}\neq 0$ [Fig. 6(b)] compared to $\bar{n}=0$ [Fig. 6(a)].

Although the decay rate in the presence of thermal noise is enhanced by a factor of $(\frac{4}{3}\bar{n}+1)$ (for three ground states) and $(2\bar{n}+1)$ (for pure two level), the excited population cannot be emptied but reaches a finite limiting value. The thermal radiation provides continuous pumping which maintains a nonzero population in the excited state with finite internal entropy at equilibrium.

## VI. COMPARISONS WITH FOKKER-PLANCK RESULTS

All the above results correctly describe the dynamics of the momentum distribution for $|\mathbf{P}|\ll Mc$ with negligible Doppler shift. This corresponds to the early stage of the time evolution when the distribution is still narrow. As the spreading continues in thermal radiation, the maximum Doppler shift increases and the Doppler shift becomes significant. The dynamics for part of the distribution with $|\mathbf{P}|\gg\hbar\mathbf{k}_o$

should well be described the Fokker-Planck equation results of Ref. [11] while the part with $|\mathbf{P}| \ll Mc$ is still precisely described by our results. Our results can well describe the early dynamics of the cold gas but not the steady-state distribution. The steady-state distribution can be described by the solutions of Fokker-Planck equation of Ref. [11] for the probability momentum distribution $f(\mathbf{P},t)$,

$$\frac{\partial f(\mathbf{P},t)}{\partial t} = \gamma \nabla \cdot \{\mathbf{P} f(\mathbf{P},t)\} + \tfrac{1}{3} D \nabla^2 f(\mathbf{P},t), \tag{21}$$

where $\gamma \doteq (1/k_B T)(\hbar^2 k_o^2/3M)[\Gamma \bar{n}(\bar{n}+1)/2\bar{n}+1]$ is the damping rate towards thermal equilibrium and $D \doteq \hbar^2 k_o^2[\Gamma \bar{n}(\bar{n}+1)/2\bar{n}+1]$ is the diffusion coefficient. For the initial Gaussian distribution $f(\mathbf{P},0) = \Pi_{i=x,y,z}(1/\sqrt{\pi} a_i) e^{-(P_i/a_i)^2}$, Eq. (21) gives the transient solution $f(\mathbf{P},t) = \Pi_{i=x,y,z}\{1/[a_i(t)\sqrt{\pi}]\} e^{-P_i^2/a_i^2(t)}$, where $a_i(t) \doteq \sqrt{(2D/3\gamma)(1-e^{-2\gamma t}) + a_i^2 e^{-2\gamma t}}$ is the transient momentum width. The gas reaches the steady-state distribution $f(\mathbf{P},\infty) = (1/\sqrt{\pi 2D/3\gamma}) e^{-P^2/\{2D/3\gamma\}}$ with the maximum entropy and momentum width $\sqrt{2D/3\gamma}$, corresponding to the thermal radiation temperature $T = (D/\gamma 3 M k_B)$. This occurs in a very long time scale of $\gamma^{-1} \approx 10^{13}$ s ($10^6$ yr) and $3 \times 10^{11}$ s(9000 yr) for optical and infrared transitions, respectively. Thus, spontaneous emission is a very slow and ineffective mechanism of thermalization with the thermal radiation. This is not surprising because of the weak coupling between atom and radiation in free space. Physically, the presence of damping $\gamma$ is due to the higher probability of absorbing a blue-Doppler shifted thermal photon and slowed down. The thermal photons act as a ''viscous medium'' to the particles and eventually bring the gas into thermal equilibrium with thermal radiation.

For time $t \ll \gamma^{-1}$, we can expand $e^{-2\gamma t} \sim 1 - 2\gamma t$ in the transient solution and find that the change in the momentum width decreases with time as

$$a_i(t) = \sqrt{\left(\frac{4D}{3} - 2a_i^2 \gamma\right) t + a_i^2}. \tag{22}$$

Similarly, we find that the amount of momentum spreading after one decay lifetime is dependent on the initial momentum width as

$$\delta\sigma_i = \frac{2}{3}\hbar^2 k_o^2 \frac{\bar{n}(\bar{n}+1)}{2\bar{n}+1}\left(\frac{1}{a_i} - \frac{a_i}{2Mk_BT}\right). \tag{23}$$

Both Eqs. (23) and (22) are in accordance with Fig. 4(c).

## VII. CONCLUSIONS

We have solved and studied the momentum and temporal evolutions of a cold gas undergoing spontaneous emissions in a two-level system with an excited state and three degenerate ground states. Analytical solutions that are essentially exact in the cold gas regime are derived for a specific internal scheme and for the zero-temperature cases. The analytical results are combined with Fourier-transform technique to compute the time- and momentum-dependent populations. This technique provides an alternative to other methods [14] for simulation of the laser cooling process where the density-matrix elements depend on the continuous variables of time and momentum. The results of the momentum spread of cold gas in thermal radiation are computed and compared for different internal schemes, with subrecoil initial width, without thermal radiation and the different types of transitions in a pure two-level system. We confine our computation results to one dimension to bring out the essential physics. Extension of the computation results to higher dimensions is straightforward using the obtained theoretical solutions. We have pointed out the range of validity of our results and compared them to the Fokker-Planck results. Our results can well describe the cold gas regime and thus complement the results in Ref. [11].

## ACKNOWLEDGMENTS

We gratefully acknowledge the financial support of the Deutsche Forschungsgemeinschaft and the Forschergruppe Quantengase.

## APPENDIX A: LIOUVILLEAN AND GENERALIZED BLOCH EQUATIONS

The quantum dynamics of the internal and center-of-mass (c.m.) momentum states of a particle system in the thermal reservoir of temperature $T$ is fully described by the master equation $[\partial\hat{\rho}_S(t)/\partial t] = L\hat{\rho}_S(t)$ for the reduced density operator of the system $\hat{\rho}_S(t)$ where $L\hat{\rho}_S(t)$ is the dissipative Liouvillean. The Liouvillean for *multistate* system in interaction picture with the Born-Markov, dipole and rotating wave approximations has been derived using the standard method [7] as

$$\begin{aligned}
L\hat{\rho}_S(t) \doteq & -\int_0^t d\tau \sum_{i,j,\mathbf{k},\lambda,\mathbf{P}'} g_{i\mathbf{k}\lambda} g^*_{j\mathbf{k}\lambda} \{(\bar{n}_k+1) e^{-i\Delta^+_{j\mathbf{k}\mathbf{P}'}\tau} e^{i\omega_{oij}t} S_i^+ S_j |\mathbf{P}'\rangle\langle\mathbf{P}'|\hat{\rho}_S(t) + \bar{n}_k e^{i\Delta^-_{j\mathbf{k}\mathbf{P}'}\tau} e^{-i\omega_{oij}t} S_i S_j^+ |\mathbf{P}'\rangle\langle\mathbf{P}'|\hat{\rho}_S(t)\} \\
& - \int_0^t d\tau \sum_{i,j,\mathbf{k},\lambda,\mathbf{P}'} g_{i\mathbf{k}\lambda} g^*_{j\mathbf{k}\lambda} \{(\bar{n}_k+1)\hat{\rho}_S(t)|\mathbf{P}'\rangle\langle\mathbf{P}'|S_j^+ S_i e^{-i\omega_{oij}t} e^{i\Delta^+_{j\mathbf{k}\mathbf{P}'}\tau} + \bar{n}_k \hat{\rho}_S(t)|\mathbf{P}'\rangle\langle\mathbf{P}'|S_j S_i^+ e^{i\omega_{oij}t} e^{-i\Delta^-_{j\mathbf{k}\mathbf{P}'}\tau}\} \\
& + \int_0^t d\tau \sum_{i,j,\mathbf{k},\lambda,\mathbf{P}',\mathbf{P}''} g_{i\mathbf{k}\lambda} g^*_{j\mathbf{k}\lambda} \{\bar{n}_k e^{-i\Delta^+_{j\mathbf{k}\mathbf{P}''}\tau} S_i^+ \hat{\rho}_S(^{\mathbf{P}'-\hbar\mathbf{k}}_{\mathbf{P}''-\hbar\mathbf{k}}, t) S_j e^{i\omega_{oij}t} + (\bar{n}_k+1) e^{i\Delta^-_{j\mathbf{k}\mathbf{P}''}\tau} S_i \hat{\rho}_S(^{\mathbf{P}'+\hbar\mathbf{k}}_{\mathbf{P}''+\hbar\mathbf{k}}, t) S_j^+ e^{-i\omega_{oij}t}\} \\
& + \int_0^t d\tau \sum_{i,j,\mathbf{k},\lambda,\mathbf{P}',\mathbf{P}''} g_{i\mathbf{k}\lambda} g^*_{j\mathbf{k}\lambda} \{\bar{n}_k e^{i\Delta^+_{j\mathbf{k}\mathbf{P}'}\tau} S_j^+ \hat{\rho}_S(^{\mathbf{P}'-\hbar\mathbf{k}}_{\mathbf{P}''-\hbar\mathbf{k}}, t) S_i e^{-i\omega_{oij}t} + (\bar{n}_k+1) e^{-i\Delta^-_{j\mathbf{k}\mathbf{P}'}\tau} S_j \hat{\rho}_S(^{\mathbf{P}'+\hbar\mathbf{k}}_{\mathbf{P}''+\hbar\mathbf{k}}, t) S_i^+ e^{i\omega_{oij}t}\}
\end{aligned} \tag{A1}$$

with the definitions

$$\hat{\rho}_S\left(\begin{matrix}\mathbf{P}'\pm\hbar\mathbf{k}\\ \mathbf{P}''\pm\hbar\mathbf{k}\end{matrix},t\right)\doteq e^{\mp i(\omega_{\mathbf{P}'}-\mathbf{P}'')t}|\mathbf{P}'\rangle\langle\mathbf{P}'\pm\hbar\mathbf{k}|\hat{\rho}_S(t)|\mathbf{P}''\pm\hbar\mathbf{k}\rangle\langle\mathbf{P}''|,$$

$$g_{i\mathbf{k}\lambda}\doteq\mathbf{d}_i\cdot\hat{\varepsilon}_{\mathbf{k}\lambda}\sqrt{\frac{\omega_k}{2\varepsilon_o V\hbar}}=d_i\sum_{q=+,-,0}\epsilon_{\mathbf{k}\lambda q}C_{q,i}\sqrt{\frac{\omega_k}{2\varepsilon_o V\hbar}},$$

$$\Delta^{\pm}_{j\mathbf{kP}}\doteq\omega_k-\omega_{oj}-\omega_{\mathbf{P}}\pm\omega_r,$$

$$\omega_{\mathbf{P}'-\mathbf{P}''}\doteq\omega_{\mathbf{P}'}-\omega_{\mathbf{P}''},$$

where the indices $i,j$ correspond to a pair states with dipole allowed transition with energy-level spacing $\omega_{oij}\doteq\omega_{oi}-\omega_{oj}$, $\omega_{\mathbf{P}}\doteq\mathbf{P}\cdot\hat{\kappa}\omega_k/Mc$ the first-order Doppler shift, $\omega_r\doteq\hbar\omega_k^2/2Mc^2$ the recoil frequency, $\hat{\kappa}\doteq(\sin\theta\cos\phi,\sin\theta\sin\phi,\cos\theta)$ the photon unit wavevector in terms of spherical angles $\Omega\equiv(\phi,\theta)$, $\overline{n}_k\doteq(e^{\hbar\omega_k/k_BT}-1)^{-1}$ is the mean thermal photon number, $S_i\doteq|g_i\rangle\langle e_i|$ is the lowering operator for the $i$th pair of levels, $d_i$ is the reduced dipole moment, $\epsilon_{\mathbf{k}\lambda q}$ is the $q$ component of the electric field with wave vector $\mathbf{k}$ and polarization index $\lambda$, and $C_{q,i}$ the numerical factor which includes the Clebsch-Gordan coefficient and the Hönl-London factor (for molecules) [8] for the transition between the $i$th pair of levels. The change in magnetic quantum numbers $q\doteq M_{ei}-M_{gi}$ corresponds to the dipole allowed $\sigma$ transition ($q=\pm1$) and $\pi$ transition ($q=0$).

We consider a *two-level multistate* system, specifically with one excited state $|e\rangle$ with the magnetic quantum number $M_e$ and three degenerate magnetic (Zeeman) ground states $|a\rangle$, $|b\rangle$ and $|c\rangle$ with the respective magnetic quantum numbers $M_a=M_e-1$, $M_b=M_e$, and $M_c=M_e+1$. By taking the diagonal matrix elements in the momentum states in Eq. A1, we obtain the generalized Bloch equations

$$\frac{\partial\rho_{ee}(\mathbf{P},t)}{\partial t}=-\rho_{ee}(\mathbf{P},t)\sum_{j,\mathbf{k}\lambda}|g_{j\mathbf{k}\lambda}|^2(\overline{n}_k+1)\int_0^t d\tau 2\cos\Delta^{+}_{j\mathbf{kP}}\tau+\sum_{j,\mathbf{k}\lambda}|g_{j\mathbf{k}\lambda}|^2\overline{n}_k\rho_{jj}(\mathbf{P}-\hbar\mathbf{k})\times\int_0^t d\tau(e^{-i\Delta^{+}_{j\mathbf{kP}}\tau}+e^{i\Delta^{+}_{i\mathbf{kP}}\tau}),$$

$$\frac{\partial\rho_{ii}(\mathbf{P},t)}{\partial t}=-\sum_{j,\mathbf{k}\lambda}g_{i\mathbf{k}\lambda}g_{j\mathbf{k}\lambda}\overline{n}_k\int_0^t d\tau\{e^{i\Delta^{-}_{j\mathbf{kP}'}\tau}e^{-i\omega_{oij}t}\rho_{ji}(\mathbf{P},t)+\rho_{ij}(\mathbf{P},t)e^{i\omega_{oij}t}e^{-i\Delta^{-}_{j\mathbf{kP}'}\tau}\}+\sum_{\mathbf{k}\lambda}|g_{i\mathbf{k}\lambda}|^2(\overline{n}_k+1)\rho_{ee}(\mathbf{P}+\hbar\mathbf{k})\int_0^t d\tau 2\cos\Delta^{-}_{i\mathbf{kP}}\tau, \tag{A2}$$

where $i,j\in a,b,c$ and $\rho_{ij}(\mathbf{P}\pm\hbar\mathbf{k},t)\doteq\langle i,\mathbf{P}\pm\hbar\mathbf{k}|\hat{\rho}(t)|j,\mathbf{P}\pm\hbar\mathbf{k}\rangle$.

The terms $\rho_{i,j\neq i}$ are associated with the Zeeman coherences are nonvanishing only if the dipole moments are nonorthogonal, which can be realized using polarization preselection in cavity [9] and specific atomic levels which lead to spontaneously generated coherences [10].

Here, we consider the typical scheme available in a molecular system where the Zeeman coherences vanish between different transitions due to orthogonality of the vector dipole matrix elements. Thus, Eqs. (A2) reduce to the multistate coupled equations between the excited and ground populations without coherences,

$$\frac{\partial\rho_{ee}(\mathbf{P},t)}{\partial t}=\sum_{j,\mathbf{k},\lambda}|g_{j,\mathbf{k}\lambda}|^2 2\int_0^t d\tau\cos\Delta^{+}_{\mathbf{kP}}\tau\{-(\overline{n}_k+1)\rho_{ee}(\mathbf{P},t)+\overline{n}_k\rho_{jj}(\mathbf{P}-\hbar\mathbf{k},t)\},$$

$$\frac{\partial\rho_{jj}(\mathbf{P},t)}{\partial t}=\sum_{\mathbf{k},\lambda}|g_{j,\mathbf{k}\lambda}|^2 2\int_0^t d\tau\cos\Delta^{-}_{\mathbf{kP}}\tau\{-\overline{n}_k\rho_{jj}(\mathbf{P},t)+(\overline{n}_k+1)\rho_{ee}(\mathbf{P}+\hbar\mathbf{k},t)\}, \tag{A3}$$

where $\rho_{\alpha\alpha}(\mathbf{P}\pm\hbar\mathbf{k},t)\doteq\langle\alpha,\mathbf{P}\pm\hbar\mathbf{k}|\hat{\rho}(t)|\alpha,\mathbf{P}\pm\hbar\mathbf{k}\rangle$ and $j\in a,b,c$. Equations (A3) can be simply reduced to the *pure two-level* or *two-state* system which is restricted only to atoms and pure rotational dipole transitions in molecules, for example between $|J=1,M=1\rangle$ and $|J=0,M=0\rangle$.

In the isotropic free space with continuum frequency spectrum, we use $\Sigma_{\mathbf{k},\lambda}|g_{j,\mathbf{k}\lambda}|^2\ldots\rightarrow(\Gamma/2\pi)\int d\omega(\omega^3/{\omega_o}^3)\int d\Phi_j\ldots$, where $\int d\Phi_j\ldots\doteq(3/8\pi)\int_0^{2\pi}d\phi\int_0^{\pi}d\theta\Sigma_{q=0,\pm1}C^2_{q,j}N_q(\theta)\ldots$, $\Gamma\doteq(d_o^2{\omega_o}^3/3\varepsilon_o\hbar\pi c^3$, and $N_q(\theta)\doteq\delta_{q0}\sin^3\theta+\delta_{q\pm}(\sin\theta-\frac{1}{2}\sin^3\theta)$. For $t\gg1/\Delta^{\pm}_{\mathbf{kP}}$, we replace $\int_0^t d\tau\cos\Delta^{\pm}_{\mathbf{kP}}\tau\rightarrow\pi\delta(\Delta^{\pm}_{\mathbf{kP}})=\pi\delta(\omega-\omega_o-\omega_{\mathbf{P}}\pm\omega_r)$ and Eqs. (A3) become

$$\frac{\partial\rho_{ee}(\mathbf{P},t)}{\partial t}=\Gamma\frac{3}{8\pi}\int d\omega\frac{\omega^3}{{\omega_o}^3}\int_0^{2\pi}d\phi\int_0^{\pi}d\theta\sum_j\sum_{q=0,\pm1}C^2_{q,j}N_q(\theta)\delta(\Delta^{+}_{\mathbf{kP}})\left\{-(\overline{n}(\omega)+1)\rho_{ee}(\mathbf{P},t)+\overline{n}(\omega)\rho_{jj}\left(\mathbf{P}-\hat{\kappa}\frac{\hbar\omega}{c},t\right)\right\},$$

$$\frac{\partial\rho_{jj}(\mathbf{P},t)}{\partial t}=\Gamma\frac{3}{8\pi}\int d\omega\frac{\omega^3}{{\omega_o}^3}\int_0^{2\pi}d\phi\int_0^{\pi}d\theta\sum_{q=0,\pm1}C^2_{q,j}N_q(\theta)\delta(\Delta^{-}_{\mathbf{kP}})\left\{-\overline{n}(\omega)\rho_{jj}(\mathbf{P},t)+[\overline{n}(\omega)+1]\rho_{ee}\left(\mathbf{P}+\hat{\kappa}\frac{\hbar\omega}{c},t\right)\right\}. \tag{A4}$$

### APPENDIX B: ENTROPY

The center-of-mass quantum entropy $S_{cm}(t)$ can be computed from Ref. [12],

$$S_{cm}(t) \doteq -k_B \mathrm{Tr}_{cm}\{\hat{\rho}_{cm}(t)\ln\hat{\rho}_{cm}(t)\} = -k_B \sum_{\mathbf{P}} g(\mathbf{P},t)\ln g(\mathbf{P},t), \tag{B1}$$

where $\hat{\rho}$ is the density operator of the gas which includes the internal and c.m. degrees of freedom, $\hat{\rho}_{cm}(t) \doteq \mathrm{Tr}_i\{\hat{\rho}(t)\} = \Sigma_{a=e,0,\pm}\langle a|\hat{\rho}(t)|a\rangle, g(\mathbf{P},t) \doteq f(\mathbf{P},t)\Delta^3 P$ is the discretized probability $f(\mathbf{P},t) \doteq \langle \mathbf{P}|\hat{\rho}_{cm}(t)|\mathbf{P}\rangle = \rho_{ee}(\mathbf{P},t) + \Sigma_q \rho_{qq}(\mathbf{P},t)$ is the probability momentum distribution with single-particle normalization, $\int f(\mathbf{P},t)d^3P = 1$.

The internal entropy $S_i(t)$ is defined as

$$S_i(t) \doteq -k_B \mathrm{Tr}_i\{\hat{\rho}_i(t)\ln\hat{\rho}_i(t)\} = -k_B \sum_{a=e,0,\pm} \pi_{aa}(t)\ln\pi_{aa}(t), \tag{B2}$$

where $\hat{\rho}_i(t) \doteq \mathrm{Tr}_{cm}\{\hat{\rho}(t)\} = \int \langle \mathbf{P}|\hat{\rho}(t)|\mathbf{P}\rangle d^3P$, $\pi_{aa}(t) \doteq \langle a|\hat{\rho}_i(t)|a\rangle$ is the momentum summed population in state $|a\rangle$.


[1] G.S. Agarwal, *Quantum Optics*, in *Springer Tracts in Modern Physics*, edited by G. Höhler (Springer, Berlin, 1974), Vol. 70.

[2] Claude N. Cohen-Tannoudji, Rev. Mod. Phys. **70**, 707 (1998); Carl E. Wieman, David E. Pritchard, and David J. Wineland, *ibid.* **71**, S253 (1999).

[3] H. Metcalf and P. van der Straten, Phys. Rep. **244**, 203 (1994); S. Stenholm, Rev. Mod. Phys. **58**, 699 (1986).

[4] C. Adams, M. Sigel, and J. Mlynek, Phys. Rep. **240**, 143 (1994).

[5] Y. Castin, H. Wallis, and J. Dalibard, J. Opt. Soc. Am. B **6**, 2046 (1989); A. Aspect, E. Arimondo, R. Kaiser, N. Vansteenkiste, and C. Cohen-Tannoudji, *ibid.* **6**, 2112 (1989).

[6] A.B. Matsko, I. Novikova, M.O. Scully, and G.R. Welch, Phys. Rev. Lett. **87**, 133601 (2001).

[7] C. Cohen-Tannoudji, in *Frontiers in Laser Spectroscopy*, edited by R. Balian, S. Haroche, and S. Liberman (North-Holland, Amsterdam, 1977); G.S. Agarwal, in *Progress in Optics*, edited by E. Wolf (North-Holland, Amsterdam, 1973), Vol. XI, p. 40; W.H. Louisell, *Quantum Statistical Properties of Radiation* (Wiley, New York, 1973), p. 349.

[8] R.N. Zare, *Angular momentum* (Wiley, New York, 1988).

[9] A.K. Patnaik and G.S. Agarwal, Phys. Rev. A **59**, 3015 (1999).

[10] J. Javanainen, Europhys. Lett. **17**, 407 (1992).

[11] C. Cohen-Tannoudji, J. Dupont-Roc, and G. Grynberg, *Atom Photon Interactions: Basic Processes and Applications* (Wiley, New York, 1992), p. 293; Jean Dalibard, Ph.D. thesis, Université Pierre et Marie Curie, Paris, 1986, p. 74.

[12] G. Lindblad, *Non-Equilibrium Entropy and Irreversibility* (Reidel, Dordrecht, 1983).

[13] G.S. Agarwal and Sunish Menon, Phys. Rev. A **63**, 23818 (2001).

[14] Examples of computational methods are the quantum Monte Carlo [e.g., R. Blatt, W. Ertmer, P. Zoller, and J.L. Hall, Phys. Rev. A **34**, 3022 (1987); M.D. Hoogerland *et al.*, **54**, 3206 (1996)], and method used in Ref. [5].